

# Alloying effect on grain-size dependent deformation twinning in nanocrystalline Cu-Zn alloys

X.L. Ma, W.Z. Xu, H. Zhou, J.A. Moering, J. Narayan & Y.T. Zhu

To cite this article: X.L. Ma, W.Z. Xu, H. Zhou, J.A. Moering, J. Narayan & Y.T. Zhu (2015) Alloying effect on grain-size dependent deformation twinning in nanocrystalline Cu-Zn alloys, Philosophical Magazine, 95:3, 301-310, DOI: [10.1080/14786435.2014.1000418](https://doi.org/10.1080/14786435.2014.1000418)

To link to this article: <https://doi.org/10.1080/14786435.2014.1000418>



Published online: 09 Jan 2015.



Submit your article to this journal [↗](#)



Article views: 580



View related articles [↗](#)



View Crossmark data [↗](#)



Citing articles: 3 View citing articles [↗](#)

## Alloying effect on grain-size dependent deformation twinning in nanocrystalline Cu–Zn alloys

X.L. Ma<sup>a</sup>, W.Z. Xu<sup>a</sup>, H. Zhou<sup>a,b</sup>, J.A. Moering<sup>a</sup>, J. Narayan<sup>a</sup> and Y.T. Zhu<sup>a,c,\*</sup>

<sup>a</sup>Department of Materials Science and Engineering, North Carolina State University, Raleigh, NC 27695, USA; <sup>b</sup>National Engineering Research Center of Light Alloy Net Forming, Shanghai Jiao Tong University, Shanghai 200240, China; <sup>c</sup>School of Materials Science and Engineering, Nanjing University of Science and Technology, Nanjing 210094, China

(Received 17 October 2014; accepted 13 December 2014)

Grain-size dependency of deformation twinning has been previously reported in nanocrystalline face-centred-cubic metals, which results in an optimum grain-size range for twin formation. Here, we report, for the first time in experiments, the observed optimum grain sizes for deformation twins in nanocrystalline Cu–Zn alloys which slightly increase with increasing Zn content. This result agrees with the reported trend but is much weaker than predicted by stacking-fault-energy based models. Our results indicate that alloying changes the relationship between the stacking-fault and twin-fault energy and therefore affects the optimum grain size for deformation twinning. These observations should be also applicable to other alloy systems.

**Keywords:** deformation twinning; nanomaterials; alloys; grain size; stacking-fault energy

### 1. Introduction

Twinning is a widely observed deformation mode in face-centred cubic (FCC) metals and alloys with nanometre-sized (<100 nm) grains, even in metals that usually do not deform by twinning at their coarse-grained state under quasi-static strain rate and room temperature [1–7]. Twin boundaries are effective in inhibiting dislocation slip and thereby increasing yield strength in a way similar to grain boundaries (GBs) [8–11]. Meanwhile, twin boundaries are able to interact with dislocations to form steps and serve as dislocation sources for further plastic deformation [12–15]. In addition, twin boundaries can also act as effective locations for dislocation accumulation, which increases the strain hardening rate and consequently improves the ductility [2,16,17]. Therefore, deformation twinning has been found as one of the most promising strategies to simultaneously enhance the strength and ductility in FCC materials.

The benefit of twinning in enhancing mechanical properties makes it a significant issue in science and engineering of FCC nanocrystalline (NC) materials. Extensive studies have revealed that the deformation twinning is influenced by both extrinsic deformation conditions, including strain, strain rate, flow stress and temperature [18–22], and intrinsic materials characteristics such as stacking-fault energy (SFE),

---

\*Corresponding author. Email: [ytzhu@ncsu.edu](mailto:ytzhu@ncsu.edu)

general planar fault energies (GPFE), crystal orientation and grain size [2,23–26]. Recent experimental investigations have found that twinning propensity first increases then decreases with decreasing grain size in different FCC NC materials, indicating that there exists an optimal grain size window for the formation of deformation twins ( $d_{\text{op}}$ ) [27–30]. This is important to the practical design of nanomaterials for superior mechanical properties since this is the grain size window in which the twin structure is most stable [2,25,27].

In the analytical model that predicted the optimal grain size for deformation twinning, SFE is one of the most important factors that affect the optimal grain size [31,32]. The model agrees reasonably well with experimental observations in pure FCC metals [2,33]. Generally, the optimal grain size for twinning increases with decreasing SFE. The most effective way to change SFE is by alloying. However, so far there have been no systematic experimental studies on alloying effect on the optimal grain size for deformation twinning. Recent *ab initio* simulation on GPFE has uncovered some salient differences between pure metals and their alloys [34]. For example, the generally accepted relationship in pure FCC metals,  $\gamma_{\text{SF}}$  (SFE)  $\approx 2\gamma_{\text{twin}}$  (twin-fault energy), is no longer valid in their alloys due to the inhomogeneous distribution of solutes [34–36]. In other words, the configuration of grain-size effect on deformation twinning in alloys may differ from the predictions of the reported model.

In this work, Cu–Zn alloys were deformed and refined to nanometre grain sizes by high-pressure torsion (HPT). By changing the Zn compositions and deforming under identical conditions, we were able to systematically investigate the effect of alloying on grain-size dependent twinning propensity and the optimal grain size for twinning in NC materials.

## 2. Experimental method

Commercial Cu-10wt.%Zn, Cu-15wt.%Zn and Cu-30wt.%Zn plates with coarse grains were punched into  $\phi$ -10 mm disks, which were subjected to HPT for six revolutions with an imposed pressure of 1GPa at 1.5 rpm. The grain-size distributions were characterized in a JEOL-2010F transmission electron microscope (TEM) operated at 200 kV. Statistical analysis of deformation twins was conducted by high-resolution electron microscopy (HREM) observation of at least 170 grains in each sample. All TEM samples were cut from the very edge of as-HPTed disks as this was the region with the greatest degree of grain refinement. Samples were subsequently mechanical polished and ion milled. Theoretical critical stress and the optimal grain size for twinning in each alloy were calculated through previously proposed model based on pure metals, which helps to identify the influence of alloying and establish correlations with the experimental results.

## 3. Results and discussion

Figure 1 shows the typical bright-field TEM images and diffraction patterns of three alloys after HPT for six revolutions at room temperature. All samples have achieved significant grain refinement to nanoscale when compared to raw materials. The simple shear strain at the edge of our samples is sufficient enough to make microstructure

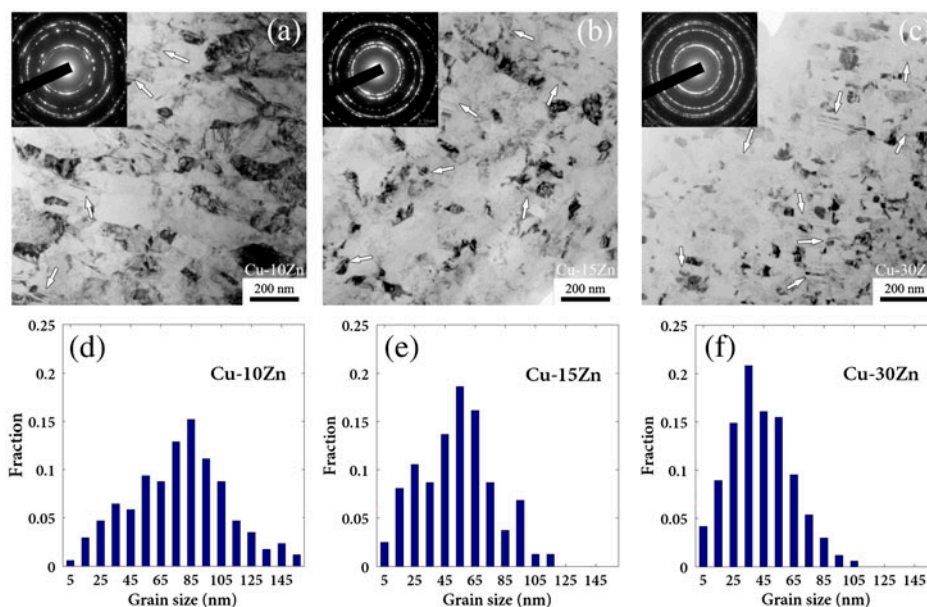


Figure 1. (colour online) Bright-field TEM images of (a) Cu-10Zn, (b) Cu-15Zn and (c) Cu-30Zn show HPTed microstructures containing nanosize grains and deformation twins. Insets are corresponding selected area diffraction patterns. Statistical grain-size distributions of (d) Cu-10Zn, (e) Cu-15Zn and (f) Cu-30Zn show considerable proportions of nanograins for statistical analysis.

evolution to reach equilibrium when compared with previous studies [37]. But the microstructure morphologies vary slightly in different alloys. Some elongated grains are present in Cu-10Zn while the major constituent of Cu-30Zn microstructure is equiaxed grain. This is probably ascribed to their various SFEs, which will determine different capabilities of the formation of subgrain boundaries during the deformation and refinement [38,39]. It is worth noting that the deformation twins are frequently seen in as-processed samples (marked by white arrow in Figure 1). Insets are corresponding diffraction patterns. The presence of cluster diffraction spots and rings imply almost random misorientations of grains. Despite the minor discontinuity of diffraction rings, there is no prevailing texture along the observation direction. These results are consistent with the previous result of Cu after high strain torsion [37]. Figure 1(d)–(f) are statistical grain-size distributions in each material, indicating the average grain sizes are 77, 53 and 43 nm for Cu-10Zn, Cu-15Zn and Cu-30Zn, respectively. Grain size is determined by geometric mean of its long and short dimensions. The difference among effectiveness of refinement in alloys is related to their SFEs [39–42]. Note that the large grain-size range from below 10 nm to more than 100 nm allow us to perform careful statistical analysis of grain size dependent twinning in each material.

HREM images in Figure 2(a)–(c) depict three typical twin morphologies in Cu–Zn alloys, which were counted as deformation twins in statistical analysis. Figure 2(a) shows a deformation twin with both ends terminated at GBs (as indicated by white asterisks in the inset), which is typical in NC materials. Non-equilibrium GBs with high

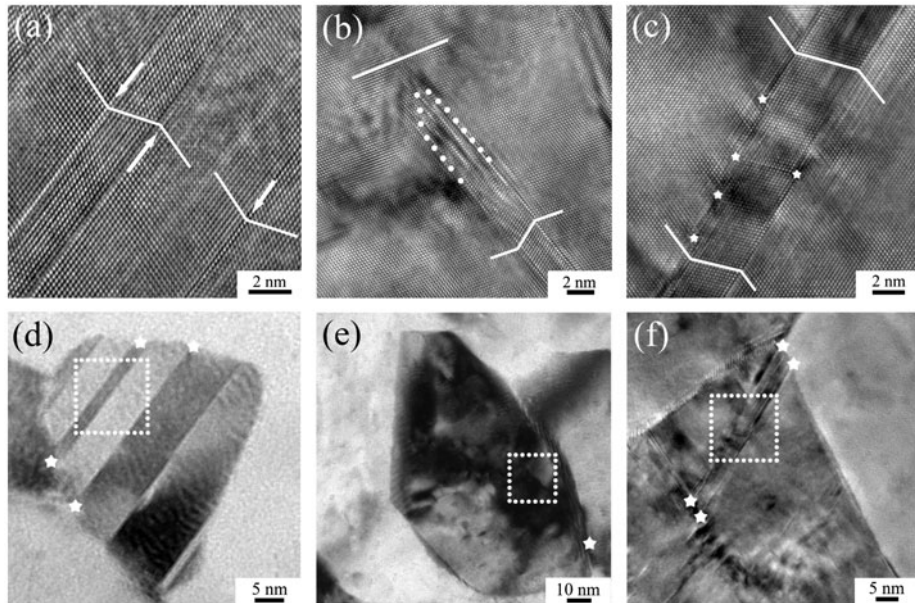


Figure 2. Typical twinning morphologies in deformed NC Cu–Zn alloys: (a) Deformation twins across the whole grain. (b) Deformation twin terminated in the grain interior. (c) Deformation twin highly interacted with other defects. Specific locations in corresponding nanograins are shown in (d)–(f). Note all twins are bounded by GBs, as shown by asterisks.

energy usually exist in severely deformed NC samples [43,44]. They can serve as sources for partial emissions and promote the nucleation of deformation twins by readily overcoming the barrier of unstable SFE and unstable twin-fault energy [2,45–47]. Therefore, the other two important parameters in GPFE curve: SFE ( $\gamma_{\text{SF}}$ ) and twin-fault energy ( $\gamma_{\text{twin}}$ ) will dominate the twinning propensity in such scenario [32,48]. Figure 2(b) shows a deformation twin terminated in the grain interior (marked by white dots). Such features appear in these samples and provide evidence for the formation mechanism of partial emission from GB [47], which is the basis for following model analysis. Figure 2(c) illustrates a deformation twin with migrated coherent twin boundary that was formed by interactions with other defects such as Shockley partials. As mentioned in the introduction, twin boundaries can also act as defect source to emit Shockley partials. Figure 2(d)–(f) demonstrate specific locations (dotted squares) of these three deformation twins at corresponding nanograins. Note that all of them are bounded by GBs (as marked by asterisks), which is the most frequently observed case in this study. This provides the fundamental basis for the semi-quantitative model which will be discussed later. It should also be clarified that not all twin structures in FCC could be revealed on any single  $\langle 110 \rangle$  zone axis under HREM because only those with the right orientation can be observed [2]. However, statistical results of deformation twins from large samples are still informative and qualitative comparisons are valid.

Figure 3 shows the statistical histogram of randomly observed nanograins and those with deformation twins, as well as the corresponding fractions of grains with

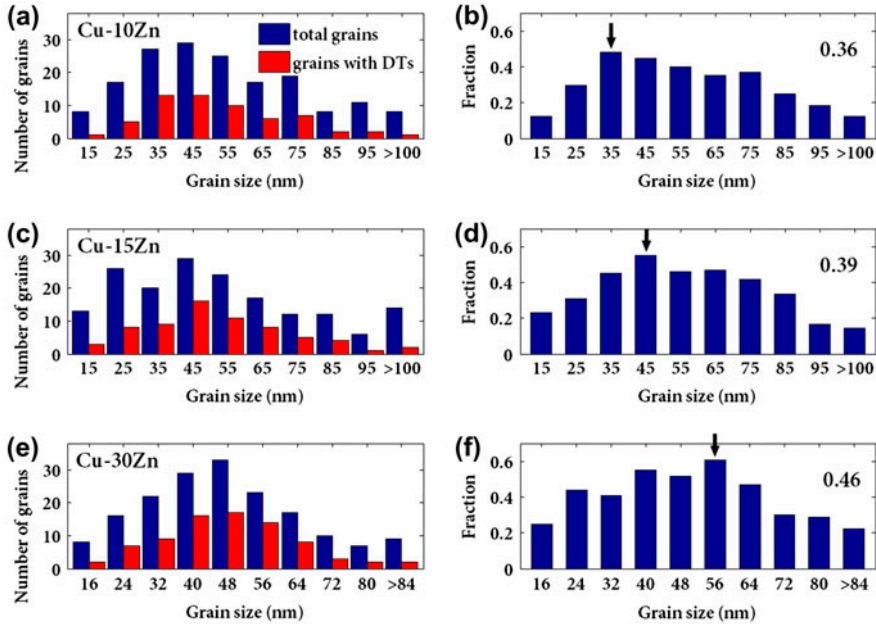


Figure 3. (colour online) Statistical analysis of randomly observed nanograins and their twinning propensities. Grain-size distributions of all observed grains (blue bar) and those with twins (red bar) in (a) Cu-10Zn, (c) Cu-15Zn, (e) Cu-30Zn. Corresponding fractions of grains with twins in (b) Cu-10Zn, (d) Cu-15Zn, (f) Cu-30Zn, including total fraction (number at top right) and those of each size region (blue bar).

deformation twins vs. grain size. In order to keep the consistency of all statistical results, additional precautions are taken to leave out those grains with severely lenticular shape (i.e. long dimension/short dimension  $> 2$ ). As a result, the total fraction of twinned grains, which can be used as an indicator of twinning propensity, increases (0.36–0.46) with increasing Zn content, which is also consistent with GPFE effect on twinning [36,49,50]. Fraction plots (Figure 3(b), (d), and (f)) also indicate a similar trend of the effect of alloying. In all three NC alloys, with decreasing grain size, the twinning propensity first increases and then decreases after certain grain sizes, i.e. there is an optimum grain size  $d_{op}$  for twinning of each alloy. The  $d_{op}$  for twinning is estimated by the location of fraction peak (black arrows in Figure 3), showing 35, 45 and 56 nm for Cu-10Zn, Cu-15Zn and Cu-30Zn, respectively. This indicates an increase in  $d_{op}$  with increasing Zn content, which has never been systematically reported before.

An analytical model has been developed to analyze the grain size effect on twinning propensity in FCC NC materials [31,32]. This model is based on classical dislocation theory and the assumption that leading Shockley partials are readily emitted from energetic GBs, which agrees with the case in this work. The critical stresses for twin nucleation ( $\tau_{twin}$ ) and trailing partial ( $\tau_{trail}$ ) to remove the first twin partial are expressed as (take screw system as an example [32]).

$$\tau_{\text{twin}} = \frac{Ga}{2\sqrt{6}\pi d \sin \alpha} \ln \frac{\sqrt{2}d}{a} \quad (1)$$

$$\tau_{\text{trail}} = \frac{\sqrt{6}}{\cos(\alpha - 30^\circ)} \left[ \frac{Ga(8 - 5\nu)}{48\pi(1 - \nu)d} \ln \frac{\sqrt{2}d}{a} - \frac{\gamma_{\text{SF}}}{a} \right] \quad (2)$$

where  $G$  is the shear modulus,  $\nu$  is the Poisson's ratio,  $\gamma_{\text{SF}}$  is the SFE,  $\alpha$  is the angle between the applied shear stress and the dislocation line,  $a$  is the lattice parameter,  $d$  is the grain size. Deformation twins are statistically promoted under the condition of  $\tau_{\text{twin}} < \tau_{\text{trail}}$ . Assuming the grains are randomly oriented and the orientation distribution are the same for grains in all size ranges, the optimum grain size for twinning  $d_{\text{op}}$  can be obtained by solving:

$$\frac{d_{\text{op}}}{\ln(\sqrt{2}d_{\text{op}}/a)} = \frac{9.69 - \nu}{253.66(1 - \nu)} \frac{Ga^2}{\gamma_{\text{SF}}} \quad (3)$$

The parameters used in model calculations are listed in Table 1 [51,52]. The comparison between model calculations and the experimental results is summarized in Figure 4. It can be concluded that the trend of alloying effect on optimum grain size for deformation twinning ( $d_{\text{op}}$ ) is consistent in models and experimental observations:  $d_{\text{op}}$  increases with the increase in Zn content. However, experimental results indicate a weaker effect than predicted by calculations. For Cu-30Zn,  $d_{\text{op}}$  is only around 56 nm, which is a much smaller increase than predicted by models (144 nm). The mechanisms underneath these two features are elucidated below.

First, increase in solute contents leads to larger optimum grain size for deformation twinning. As indicated in the model,  $d_{\text{op}}$  is determined when  $\tau_{\text{twin}}$  and  $\tau_{\text{trail}}$  are equivalent. It can be inferred from Equations (1) and (2) that SFE primarily affects  $\tau_{\text{trail}}$  by eliminating the formed stacking fault. Therefore, when SFE is decreased, more stress is required to remove the generated fault, i.e. higher  $\tau_{\text{trail}}$ . In contrast, most other material parameters, like shear modulus, Poisson's ratio and lattice parameter, are similar in the same series of alloys, as seen in Table 1. Consequently, as shown in solid plots of Figure 5, more solutes in alloys will cause the shift of  $d_{\text{op}}$  to higher region by decreasing SFE.

Second, the shift of  $d_{\text{op}}$  is not as severe as speculated by model calculations. We note that the analytical model originates from pure FCC metals. The quoted relation in this analysis is  $\gamma_{\text{SF}} \approx 2\gamma_{\text{twin}}$ , which is derived from hard-ball models and applicable to most pure FCC metals [53,54]. In reality, solute atoms are not homogeneously distributed in alloys. They prefer to locally reside near or away to the planar fault, i.e. the well-known Suzuki effect [53,55]. As a result, recent *ab initio* calculations have revealed that actual alloy systems deviate from this relationship [34,36,56], namely

Table 1. Parameters and results in calculations of the model [51,52].

Material	$\gamma_{\text{SF}}$ (mJ/m <sup>2</sup> )	$a$ (Å)	$G$ (GPa)	$\nu$	$d_{\text{op}}$ (nm)
Cu10Zn	35	3.64	44	0.307	44
Cu15Zn	25	3.65	44	0.307	72
Cu30Zn	14	3.69	40	0.375	144

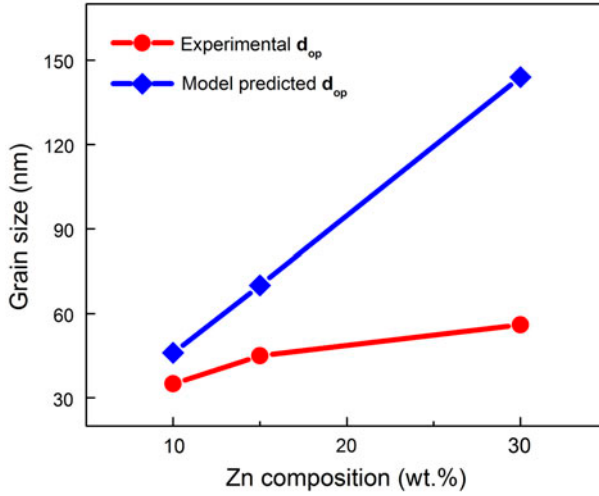


Figure 4. (colour online) Summary of experimental results and model predictions of optimum grain sizes ( $d_{op}$ ) for deformation twinning in different nanocrystalline Cu–Zn alloys vs. their Zn compositions.

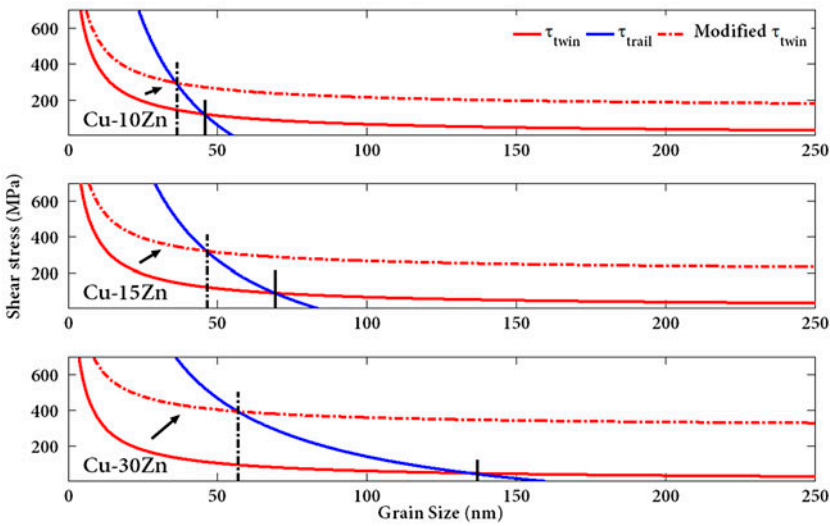


Figure 5. (colour online) Model-based stress calculation (solid lines) of twinning partial ( $\tau_{twin}$ ) and trailing partial ( $\tau_{trail}$ ) and resulted optimum grain sizes ( $d_{op}$ ) for deformation twinning in Cu–Zn alloys. Dash-dot curves schematically represent the modifications due to the inequality of  $\gamma_{SF} \neq 2\gamma_{twin}$  in alloy systems and therefore modified optimum grain sizes  $d_{op}$ .

$$\gamma_{SF} \neq 2\gamma_{twin} \tag{4}$$

For example,  $2\gamma_{twin}$  is higher than the intrinsic SFE  $\gamma_{SF}$  when Cu is alloyed with Al atoms [36,57]. In addition, simulations also implicate that this discrepancy becomes

more significant with increasing Al composition [56]. For materials in our studies, previous work has indicated the Suzuki segregation is operative even under room temperature in  $\alpha$ -brass alloy [58], proving the validity of Equation (4) in Cu–Zn alloys here. Therefore, one can envision that the energy barrier to form a deformation twin (two interfaces, i.e.  $2\gamma_{\text{twin}}$ ) is not exactly identical to that of erasing a single stacking fault ( $\gamma_{\text{SF}}$ ), especially for the highly alloyed materials (Cu-30Zn). Hence, the above-mentioned element-based model requires modifications to incorporate alloying effects. We are currently working on this issue and intend to publish the modified model in the future. Here, we demonstrate a qualitative modification. As schematically presented in the dash-dot plots in Figure 5, the change of  $\tau_{\text{twin}}$  curve results in the shift of  $d_{\text{op}}$ . Based on the experimental results,  $2\gamma_{\text{twin}}$  should be larger than  $\gamma_{\text{SF}}$  when Zn is locally segregated around planar fault, i.e.  $d_{\text{op}}$  shift to small size in each alloy. Since this effect could be amplified with increasing solute composition due to more chance of preferential and inhomogeneous segregations [56], it is reasonable for Cu30Zn to exhibit maximum deviation of  $d_{\text{op}}$  from model predictions (see the trend in Figures 4 and 5).

#### 4. Conclusion

In summary, deformation-twinning propensities in NC Cu–Zn alloys were systematically studied by HREM. Statistical results reveal a significant grain-size and inverse grain-size effect on twinability in all alloys, indicating an optimal grain size window for deformation twinning in nanograins. Also, alloying is found to affect the optimum grain size for twinning, making it deviate from what is predicted by an analytical model developed for pure FCC metals, where the twin boundary energy is assumed to be half of the stacking fault energy. However, in an alloy system, this assumption of energy relationship is no longer valid, which is the primary reason for the observed deviation. These observations should be applicable to other alloy systems.

#### Acknowledgements

The authors acknowledge the use of Analytical Instrumentation Facility (AIF) at North Carolina State University, which is supported by the State of North Carolina and the National Science Foundation.

#### Funding

This work was supported by the National Science Foundation of the USA [grant number DMR-1104667].

#### References

- [1] J.W. Christian and S. Mahajan, *Prog. Mater. Sci.* 39 (1995) p.1.
- [2] Y.T. Zhu, X.Z. Liao and X.L. Wu, *Prog. Mater. Sci.* 57 (2012) p.1.
- [3] I.J. Beyerlein, X. Zhang and A. Misra, *Annu. Rev. Mater. Res.* 44 (2014) p.329.
- [4] C.X. Huang, K. Wang, S.D. Wu, Z.F. Zhang, G.Y. Li and S.X. Li, *Acta Mater.* 54 (2006) p.655.

- [5] Y.T. Zhu, X.Z. Liao, X.L. Wu and J. Narayan, *J. Mater. Sci.* 48 (2013) p.4467.
- [6] F. Wu, Y.T. Zhu and J. Narayan, *Mater. Res. Lett.* 2 (2013) p.63.
- [7] X.Z. Liao, Y.H. Zhao, S.G. Srinivasan, Y.T. Zhu, R.Z. Valiev and D.V. Gunterov, *Appl. Phys. Lett.* 84 (2004) p.592.
- [8] L. Lu, X. Chen, X. Huang and K. Lu, *Science* 323 (2009) p.607.
- [9] P. Gu, M. Dao and Y. Zhu, *Philos. Mag.* 94 (2014) p.1249.
- [10] L. Lu, R. Schwaiger, Z.W. Shan, M. Dao, K. Lu and S. Suresh, *Acta Mater.* 53 (2005) p.2169.
- [11] Y.F. Shen, L. Lu, Q.H. Lu, Z.H. Jin and K. Lu, *Scripta Mater.* 52 (2005) p.989.
- [12] E. Ma, Y.M. Wang, Q.H. Lu, M.L. Sui, L. Lu and K. Lu, *Appl. Phys. Lett.* 85 (2004) p.4932.
- [13] Y.M. Wang, F. Sansoz, T. LaGrange, R.T. Ott, J. Marian, T.W. Barbee Jr and A.V. Hamza, *Nat. Mater.* 12 (2013) p.697.
- [14] J. Wang, N. Li, O. Anderoglu, X. Zhang, A. Misra, J.Y. Huang and J.P. Hirth, *Acta Mater.* 58 (2010) p.2262.
- [15] Y.T. Zhu, X.L. Wu, X.Z. Liao, J. Narayan, L.J. Kecskés and S.N. Mathaudhu, *Acta Mater.* 59 (2011) p.812.
- [16] Y.H. Zhao, X.Z. Liao, S. Cheng, E. Ma and Y.T. Zhu, *Adv. Mater.* 18 (2006) p.2280.
- [17] K. Lu, L. Lu and S. Suresh, *Science* 324 (2009) p.349.
- [18] G.T. Gray III, *Acta Metall.* 36 (1988) p.1745.
- [19] Y. Cao, Y.B. Wang, X.Z. Liao, M. Kawasaki, S.P. Ringer, T.G. Langdon and Y.T. Zhu, *Appl. Phys. Lett.* 101 (2012) p.231903.
- [20] R.J. McCabe, I.J. Beyerlein, J.S. Carpenter and N.A. Mara, *Nat. Commun.* 5 (2014) p.3806.
- [21] W.S. Zhao, N.R. Tao, J.Y. Guo, Q.H. Lu and K. Lu, *Scripta Mater.* 53 (2005) p.745.
- [22] G.H. Xiao, N.R. Tao and K. Lu, *Scripta Mater.* 59 (2008) p.975.
- [23] H. Swygenhoven, P.M. Derlet and A.G. Frøseth, *Nat. Mater.* 3 (2004) p.399.
- [24] M.A. Meyers, O. Vöhringer and V.A. Lubarda, *Acta Mater.* 49 (2001) p.4025.
- [25] S. Ni, Y.B. Wang, X.Z. Liao, H.Q. Li, R.B. Figueiredo, S.P. Ringer, T.G. Langdon and Y.T. Zhu, *Phys. Rev. B* 84 (2011) p.235401.
- [26] Z.W. Wang, Y.B. Wang, X.Z. Liao, Y.H. Zhao, E.J. Lavernia, Y.T. Zhu, Z. Horita and T.G. Langdon, *Scripta Mater.* 60 (2009) p.52.
- [27] X.L. Wu and Y.T. Zhu, *Phys. Rev. Lett.* 101 (2008) p.025503.
- [28] Q. Yu, Z.W. Shan, J. Li, X. Huang, L. Xiao, J. Sun and E. Ma, *Nature* 463 (2010) p.335.
- [29] J.Y. Zhang, G. Liu, R.H. Wang, J. Li, J. Sun and E. Ma, *Phys. Rev. B* 81 (2010) p.172104.
- [30] F. Wu, Y.T. Zhu and J. Narayan, *Philos. Mag.* 93 (2013) p.4355.
- [31] Y.T. Zhu, X.Z. Liao, S.G. Srinivasan, Y.H. Zhao, M.I. Baskes, F. Zhou and E.J. Lavernia, *Appl. Phys. Lett.* 85 (2004) p.5049.
- [32] Y.T. Zhu, X.Z. Liao, S.G. Srinivasan and E.J. Lavernia, *J. Appl. Phys.* 98 (2005) p.034319.
- [33] V.S. Boyko and R.Y. Kezerashvili, *J. Phys. Chem. Solids* 75 (2014) p.1119.
- [34] D. Finkenstadt and D.D. Johnson, *Phys. Rev. B* 73 (2006) p.024101.
- [35] Y.F. Wen and J. Sun, *Scripta Mater.* 68 (2013) p.759.
- [36] S. Kibey, J.B. Liu, D.D. Johnson and H. Sehitoglu, *Appl. Phys. Lett.* 89 (2006) p.191911.
- [37] T. Hebesberger, H.P. Stüwe, A. Vorhauer, F. Wetscher and R. Pippan, *Acta Mater.* 53 (2005) p.393.
- [38] Y.H. Zhao, X.Z. Liao, Y.T. Zhu, Z. Horita and T.G. Langdon, *Mater. Sci. Eng. A* 410–411 (2005) p.188.
- [39] Y.B. Wang, X.Z. Liao, Y.H. Zhao, E.J. Lavernia, S.P. Ringer, Z. Horita, T.G. Langdon and Y.T. Zhu, *Mater. Sci. Eng. A* 527 (2010) p.4959.
- [40] C.X. Huang, W. Hu, G. Yang, Z.F. Zhang, S.D. Wu, Q.Y. Wang and G. Gottstein, *Mater. Sci. Eng. A* 556 (2012) p.638.

- [41] Y.H. Zhao, Y.T. Zhu, X.Z. Liao, Z. Horita and T.G. Langdon, *Mater. Sci. Eng. A* 463 (2007) p.22.
- [42] L. Balogh, T. Ungár, Y. Zhao, Y.T. Zhu, Z. Horita, C. Xu and T.G. Langdon, *Acta Mater.* 56 (2008) p.809.
- [43] A.P. Zhilyaev and T.G. Langdon, *Prog. Mater. Sci.* 53 (2008) p.893.
- [44] J.Y. Huang, Y.T. Zhu, H. Jiang and T.C. Lowe, *Acta Mater.* 49 (2001) p.1497.
- [45] X.L. Wu, Y.T. Zhu and E. Ma, *Appl. Phys. Lett.* 88 (2006) p.121905.
- [46] X.Z. Liao, J.Y. Huang, Y.T. Zhu, F. Zhou and E.J. Lavernia, *Philos. Mag.* 83 (2003) p.3065.
- [47] Y.T. Zhu, X.L. Wu, X.Z. Liao, J. Narayan, S.N. Mathaudhu and L.J. Kecskés, *Appl. Phys. Lett.* 95 (2009) p.031909.
- [48] S. Kibey, J.B. Liu, D.D. Johnson and H. Sehitoglu, *Appl. Phys. Lett.* 91 (2007) p.181916.
- [49] N. Bernstein and E.B. Tadmor, *Phys. Rev. B* 69 (2004) p.094116.
- [50] L. Wei, L. Song, H. Qing-Miao K. Se Kyun, J. Börje and V. Levente, *J. Phys.: Condens. Matter.* 26 (2014) p.265005.
- [51] P.C. Gallaghe, *Metall. Trans.* 1 (1970) p. 2429.
- [52] J.R. Davis, *Properties and Selection: Nonferrous Alloys and Special-Purpose Materials*, ASM International, Novelty, OH, 1990.
- [53] J.P. Hirth and J. Lothe, *Theory of Dislocations*, Wiley, New York, 1982.
- [54] Z.H. Jin, S.T. Dunham, H. Gleiter, H. Hahn and P. Gumbsch, *Scripta Mater.* 64 (2011) p.605.
- [55] H. Suzuki, *J. Phys. Soc. Jpn.* 17 (1962) p.322.
- [56] S.A. Kibey, L.L. Wang, J.B. Liu, H.T. Johnson, H. Sehitoglu and D.D. Johnson, *Phys. Rev. B* 79 (2009) p.214202.
- [57] L.E. Murr, *Interfacial Phenomena in Metals and Alloys*, Addison-Wesley, Advanced Book Program, Reading, MA, 1975.
- [58] M.L. Rudee and R.A. Huggins, *Philos. Mag.* 11 (1965) p.539.